Reactive uptake of HONO on aluminium oxide surface

ARTICLE *in* JOURNAL OF PHOTOCHEMISTRY AND PHOTOBIOLOGY A CHEMISTRY · DECEMBER 2012

Impact Factor: 2.5 · DOI: 10.1016/j.jphotochem.2012.09.018

3 AUTHORS:

Manolis N Romanias
Ecole des Mines de Douai
25 PUBLICATIONS **99** CITATIONS
SEE PROFILE

Atallah El Zein
Université du Littoral Côte d'Opale (ULCO)
13 PUBLICATIONS **119** CITATIONS
SEE PROFILE

Yuri Bedjanian
CNRS Orleans Campus
67 PUBLICATIONS **861** CITATIONS
SEE PROFILE

Journal of Photochemistry and Photobiology A: Chemistry 250 (2012) 50–57

Contents lists available at SciVerse ScienceDirect

Journal of Photochemistry and Photobiology A: Chemistry

journal homepage: www.elsevier.com/locate/jphotochem

Reactive uptake of HONO on aluminium oxide surface

Manolis N. Romanias, Atallah El Zein, Yuri Bedjanian *

Institut de Combustion, Aérothermique, Réactivité et Environnement (ICARE), CNRS, 45071 Orléans Cedex 2, France

ARTICLE INFO

Article history:
Received 11 July 2012
Received in revised form 4 September 2012
Accepted 20 September 2012
Available online 13 October 2012

Keywords:
Al_2O_3
HONO
UV irradiation
Heterogeneous reaction
Uptake coefficient
Products

ABSTRACT

Kinetics and products of the interaction of HONO with solid films of Al_2O_3 were investigated under dark and UV irradiation conditions using a low pressure flow reactor (1–10 Torr) combined with a modulated molecular beam mass spectrometer for monitoring of the gaseous species involved. The reactive uptake of HONO to Al_2O_3 was studied as a function of HONO concentration ($[HONO]_0 = (0.6–3.5) \times 10^{12}$ molecule cm^{-3}), relative humidity ($RH = 1.4 \times 10^{-4}$ to 35.4%), temperature ($T = 275–320$ K) and UV irradiation intensity ($J_{NO_2} = 0.002–0.012\ s^{-1}$). The measured reactive uptake coefficient was independent of the HONO concentration and temperature. In contrast, the relative humidity (RH) was found to have a strong impact on the uptake coefficient: $\gamma = 4.8 \times 10^{-6}(RH)^{-0.61}$ and $\gamma = 1.7 \times 10^{-5}(RH)^{-0.44}$ under dark conditions and on irradiated surface ($J_{NO_2} = 0.012\ s^{-1}$), respectively (γ calculated with BET surface area, 30% conservative uncertainty). NO_2 and NO were observed as products of the HONO reaction with Al_2O_3 surface with yields of 40 ± 6 and 60 ± 9%, respectively, independent of relative humidity, temperature, concentration of HONO and UV irradiation intensity under experimental conditions used. The HONO uptake on mineral aerosol (calculated with uptake data for HONO on Al_2O_3 surface) appears to be of minor importance compared with other HONO loss processes in the boundary layer of the earth atmosphere.

1. Introduction

Nitrous acid (HONO) is an important atmospheric species representing a significant daytime photochemical source of OH radical, the major atmospheric oxidant. Therefore, HONO affects the HO_x and NO_x budgets, which are the two key groups of species involved in ozone formation, and subsequently in the oxidative capacity of the troposphere [1–3]. Because of its rapid photolysis during daytime, elevated concentrations of HONO have been observed only at night, ranging from a few ppbv at polluted sites to 70 pptv in the Arctic [4,5]. In the clean troposphere during daytime, the steady state concentrations of HONO range from 100 to 500 pptv [3,6]. The mechanisms of HONO formation in the atmosphere are still not completely understood. One current issue in the chemistry of HONO is that models fail to reproduce unexpectedly high daytime concentrations of HONO observed in the field studies, suggesting the existence of new, yet unknown, daytime sources of HONO [7]. Heterogeneous processes, including those on humid surfaces, being thought to be the major source of HONO in the atmosphere, were intensively studied in the laboratory and several mechanisms of HONO formation on aerosol and ground surfaces have been proposed [7].

In competition with heterogeneous HONO formation the atmospheric aerosol can also act as a sink for gaseous HONO, probably, hardly competitive with HONO photolysis during the day, however potentially important during night-time. The kinetic and mechanistic data on HONO interaction with different surfaces seems to be very useful, not only for atmospheric implications but also for laboratory studies of the HONO forming heterogeneous processes where secondary surface reactions of HONO may have an impact on the occurring chemistry and final HONO yields. The available information on the nature, rate and products of HONO interaction with solid surfaces of atmospheric interest is very scarce and seems to be limited to a few studies carried out with ice [2,8–11] and soot surfaces [12,13]. In addition, there have been several studies of the loss of HONO on "laboratory" surfaces such as Pyrex [14,15] and borosilicate glass [16].

The present paper is one of the series on systematic studies of the kinetics and products of the heterogeneous interaction of HONO with mineral aerosol and its different constituents carried out in our laboratory, focusing on the reaction of HONO with Al_2O_3 surface. Aluminium oxide is the second most abundant (after SiO_2) component of mineral dust (nearly 15 wt%) and is often used as a model compound to mimic the surface reactivity of mineral aerosols.

2. Materials and methods

Solid films of Al_2O_3 were deposited on the outer surface of a Pyrex tube (0.9 cm o.d.) using a suspension of γ-Al_2O_3 (Alfa Aesar,

* Corresponding author. Tel.: +33 238255474; fax: +33 238696004.
E-mail address: yuri.bedjanian@cnrs-orleans.fr (Y. Bedjanian).

1010-6030/$ – see front matter © 2012 Elsevier B.V. All rights reserved.
http://dx.doi.org/10.1016/j.jphotochem.2012.09.018

~20 nm particle diameter) powder in ethanol. Prior to film deposition, the Pyrex tube was treated with hydrofluoric acid and washed with distilled water and ethanol. Then the tube was immersed into the suspension, withdrawn and dried with a fan heater. As a result rather homogeneous (to eye) films of Al_2O_3 were formed at the Pyrex surface. In order to eliminate the possible residual traces of ethanol, prior to uptake experiments, the freshly prepared solid samples were dried at 100–150 °C during 20–30 min under pumping. BET surface area of the aluminium oxide powder was determined using a Quantachrome – Autosorb-1-MP-6 apparatus and nitrogen as adsorbate gas and was found to be $200 \pm 40\ m^2\ g^{-1}$ in agreement with the surface area range 100–200 $m^2\ g^{-1}$ given by the supplier.

The interaction of HONO with solid Al_2O_3 films was studied at 1–10 Torr total pressure (He being used as a carrier gas) using the flow tube technique with mass spectrometric detection of the gaseous species involved. The experimental equipment and approach used for the kinetic measurements were described in previous publications from this group [12,17,18]. The main reactor (Fig. S1, Supplementary data) consisted of a Pyrex tube (40 cm length and 2.4 cm i.d.) with a jacket for the thermostated liquid circulation. Experiments were carried out using a coaxial configuration of the flow reactor with movable central injector: the Pyrex tube with deposited sample was introduced into the main reactor along its axis. The coated tube could be moved relative to the outer tube of the injector that allowed the variation of the solid film length exposed to gas phase reactant and consequently of the reaction time. In addition, the sample could be heated up to a few hundreds °C by means of a coaxial cylindrical heater which could be introduced inside the tube coated with the sample.

The reactor was surrounded by 6 lamps (Sylvania BL350, 8 W, 315–400 nm with peak at 352 nm). The actinic flux inside the reactor was not measured in the present study, however, in order to characterize the irradiance intensity in the reactor we have directly measured the NO_2 photolysis frequency, J_{NO_2}, as a function of the number of lamps switched on. The values of J_{NO_2} were found to be between 0.002 and 0.012 s^{-1} for 1–6 lamps switched on, respectively [18].

HONO was generated via heterogeneous reaction of HCl with $NaNO_2$:

$$HCl + NaNO_2 \rightarrow HONO + NaCl$$

HCl diluted in He was flowed through a column containing $NaNO_2$ crystals, and heterogeneously formed HONO was injected through the reactor side arm and detected at its parent peak as $HONO^+$ ($m/z = 47$). Under the experimental conditions used this source of HONO was found to be free of residual concentration of HCl. Monitoring of the HCl concentration by mass spectrometry confirmed that HCl was completely consumed in reaction with $NaNO_2$ and did not reach the main reactor. This HONO source is known to be free of NO_2 and HNO_3 [19]. Indeed, in the present work, no signals were detected at $m/z = 46$ (NO_2^+), 62 (NO_3^+), and 63 (HNO_3^+) when HONO was present in the reactor. However, measurable concentration of NO coming from the HONO source was detected (10–20% of [HONO]) in agreement with the results of a previous study [19]. The method used for the measurements of the absolute concentrations of HONO consisted of chemical conversion of HONO to NO_2 via the fast reaction with F atoms with subsequent detection and measurement of NO_2 concentration formed [19]:

$$F + HONO \rightarrow HF + NO_2$$

H_2O was introduced into the reactor from a bubbler containing thermostated ($T = 298$ K) deionised water. The concentrations of H_2O in the reactor were determined by calculating the H_2O flow rate from the total (H_2O + He) and H_2O vapour pressures in H_2O bubbler and the measured flow rate of He through the bubbler. The concentrations of the other stable species, in particular those of the reaction products NO and NO_2, were calculated from their flow rates obtained from the measurements of the pressure drop in calibrated volume flasks with the species diluted in helium. All species were detected at their parent peaks. NO_2 and HONO were found to contribute to the mass peak $m/z = 30$, parent peak of NO, due to their fragmentation in the ion source of the mass spectrometer, which was operated at 25–30 eV. To this end, the contributions of both compounds to the signal recorded at $m/z = 30$, were determined and subtracted from the total signal.

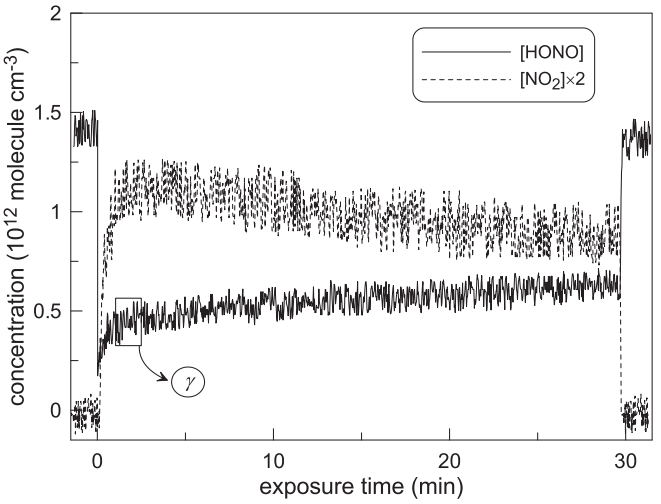

Fig. 1. Time-dependent HONO loss and NO_2 formation in reaction of HONO with Al_2O_3 surface: $T = 300$ K, dry conditions, Al_2O_3 sample mass = 0.28 mg $cm^{-1} \times 5$ cm.

3. Results

3.1. Kinetics of HONO consumption and products formation

Typical behaviour of the concentration of HONO upon Al_2O_3 sample introduction into the reaction zone (in contact with HONO, $t = 0$) is shown in Fig. 1. Three different regimes can be identified for the dependence of [HONO] upon exposure time: fast initial consumption followed by a rapid decrease of the HONO loss rate ($t = 0$–2 min) to quasi steady state, which in turn slowly decreases with time. When the sample was withdrawn from the reaction zone ($t = 30$ min, Fig. 1), i.e. when HONO was no longer in contact with the Al_2O_3 surface, the HONO concentration was found to increase rapidly, reaching its initial value. Thus, no additional HONO desorbed from the surface was observed, indicating the reactive nature of the HONO uptake. The reactive uptake of HONO was confirmed by the detection of the reaction products, NO_2 and NO. The temporal profile of NO_2 concentration is shown in Fig. 1. As can be seen, a delayed production of NO_2 was observed, the maximum NO_2 yield being reached after 2–3 min of Al_2O_3 exposure to HONO and then remained unchanged. Absolutely similar behaviour was observed for the second reaction product, NO, which is omitted in Fig. 1 for clarity. All the measurements of the reaction product concentrations presented in the paper were conducted under "stabilised" product yield conditions, i.e. upon reaching the maximum concentrations of the products ($t \geq 2$–3 min in Fig. 1).

Concerning the measurement of the uptake coefficient, the rapid initial non reactive stage of the heterogeneous interaction was not considered and the measurements were focused on the initial value of the reactive uptake coefficient as outlined in Fig. 1. The uptake

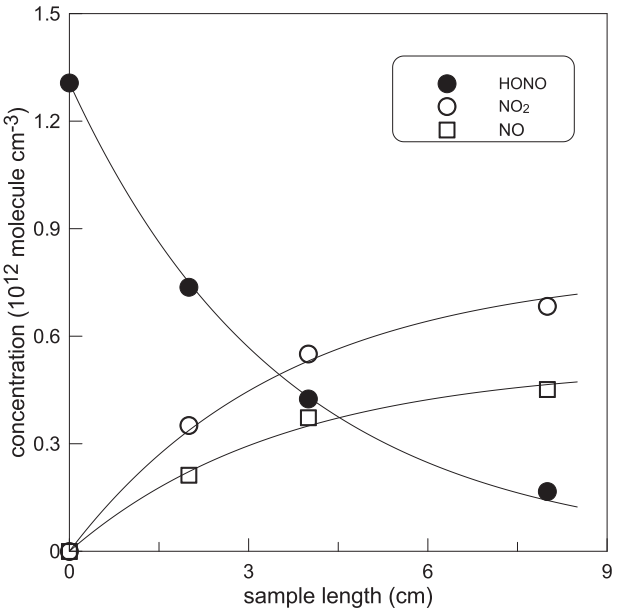

Fig. 2. Examples of kinetics of HONO consumption and products (NO and NO_2) formation on Al_2O_3 surface: $T = 300$ K, dry conditions, sample mass = 0.23 mg cm^{-1}.

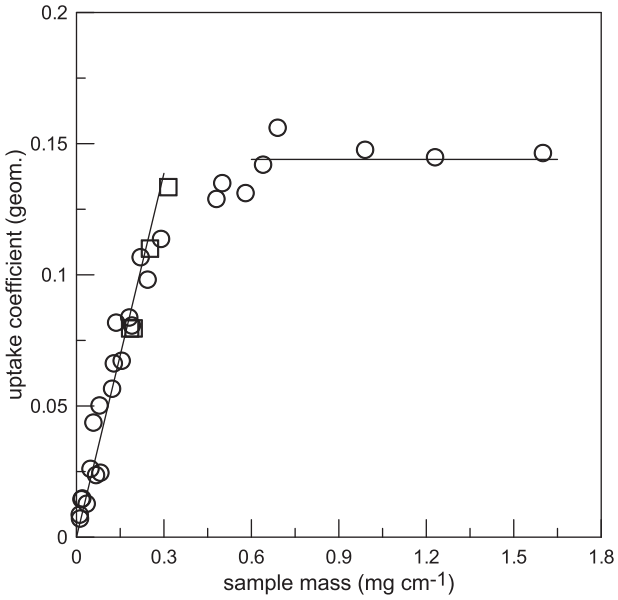

Fig. 3. Uptake coefficient of HONO on Al_2O_3 (calculated using geometric surface area) as a function of the mass of Al_2O_3 sample (per 1 cm length of the support tube): $T = 300$ K, dry conditions, [HONO] ~ 10^{12} molecule cm^{-3}. Squares represent the data obtained on irradiated surface (6 lamps on, $J_{NO_2} \cong 0.012\ s^{-1}$).

coefficient was determined as the probability of irreversible loss of HONO molecules per collision with solid surface:

$$\gamma = \frac{4k'}{\omega} \times \frac{V}{S}$$

where k' (s^{-1}) is the first order rate constant of the HONO heterogeneous loss, ω is the average molecular speed, V is the volume of the reaction zone, and S is the surface area of the Al_2O_3 coating. The rate constant of the HONO decay on the surface was calculated assuming the first-order kinetics regime, k' being determined as:

$$k' = -\frac{\mathrm{d}\ \ln([\mathrm{HONO}])}{\mathrm{d}t}$$

where t is the reaction time defined by the sample length/flow velocity ratio. An example of the HONO loss kinetics in heterogeneous reaction with Al_2O_3 surface is shown in Fig. 2. The presented data were obtained by varying the length of Al_2O_3 coating in contact with HONO, which is equivalent to varying the reaction time. The kinetics of HONO decay presented in Fig. 2 is well fitted with an exponential function (solid line) supporting the applicability of the first-order kinetics formalism. The values of the first-order rate constants, k', determined from the decays of HONO were corrected for the diffusion limitation in the HONO radial transport from the volume to the reactive surface (Bedjanian et al. [17] and references therein). For the diffusion coefficient of HONO the value of $D = 490$ Torr cm^2 s^{-1} at $T = 300$ K measured in our recent study [20] was used (assuming $T^{1.75}$-dependence of D on temperature). The diffusion corrections applied to k' ranged from a few percents up to a factor 1.6. The maximum corrections were applied to highest k' measured under dry conditions.

Fig. 2 shows also the kinetics of formation of products, NO_2 and NO. Corresponding solid lines represent fit to the experimental data according to the following equation:

$$[\mathrm{product}] = \alpha \times [\mathrm{HONO}]_0 \times (1 - \exp(-k't))$$

where k' is the first order rate constant determined from the kinetics of HONO consumption and α is the branching ratio for the product forming reaction channel. The solid lines in Fig. 2 were obtained with the values of $\alpha = 0.61$ and 0.40 for NO_2 and NO, respectively.

3.2. HONO loss rate: mass dependence

In order to determine the surface area of solid samples involved in the interaction with HONO, the HONO heterogeneous loss rate was measured as a function of the thickness of Al_2O_3 coating. The results of the measurements carried out at room temperature and under dry conditions are shown in Fig. 3 as a dependence of the uptake coefficient of HONO (γ_g, calculated with geometric "projected" surface area) on the mass of Al_2O_3 deposited per unit length of the support tube (which is equivalent to the thickness of the coating). One can note that two regimes were observed: the first one, where γ_g linearly increases upon increase of the thickness of Al_2O_3 coating, and the second one (saturation region), where γ_g is independent of the sample mass. The linear dependence of the reaction probability on mass (thickness) of the reactive film was considered as an indication that the entire surface area of the solid sample is accessible to HONO [21], and, consequently, the BET surface area should be used for calculations of the uptake coefficient. The uptake measurements in the present study were carried out with Al_2O_3 samples with masses below 0.3 mg cm^{-1}, where linear dependence of the reaction rate on sample mass was observed and BET surface area (200 m^2 g^{-1}) was used to determine γ. The linear dependence in Fig. 3 provides the following value of the uptake coefficient of HONO under dry conditions (RH ≈ 3×10^{-4}%) and $T = 300$ K:

$$\gamma = (6.5 \pm 2.0) \times 10^{-4}$$

where estimated near 30% uncertainty includes statistical one and that related to the BET surface area and to the measurements of k'. It is worth mentioning that the value obtained for γ, being calculated with BET surface area, should be considered as a lower limit of the uptake coefficient.

Three points (squares) in Fig. 3 correspond to the measurements carried out in the presence of UV irradiation (6 lamps switched on, $J_{NO_2} \cong 0.012\ s^{-1}$). One can note that the uptake data observed on irradiated Al_2O_3 surface and under dark conditions are identical, indicating the negligible impact of the irradiation on the uptake of HONO under conditions of these experiments ($T = 300$ K, dry conditions).

Table 1
Uptake coefficient of HONO on Al_2O_3 surface measured at 300 K under dark dry conditions (RH ≈ 0.0005%) as a function of the initial concentration of HONO.

$[HONO]_0$ (10^{12} molecule cm^{-3})	Sample mass (mg cm^{-1})	$\gamma \times 10^4$ [a]
0.60	0.18	5.8
1.2	0.28	4.8
1.5	0.25	5.5
2.0	0.27	5.3
3.5	0.27	4.9

[a] Estimated uncertainty of 30%.

3.3. Dependence on initial concentration of HONO

The dependence of γ on initial concentration of HONO measured at $T = 300$ K under dry conditions (RH ≈ 5×10^{-4}%) is shown in Table 1. The uptake coefficient was found to be independent of $[HONO]_0$ in the range (0.6–3.5) × 10^{12} molecule cm^{-3}. The independence of the initial uptake coefficient of the HONO concentrations could be expected, considering that HONO loss rate depends on the number of active sites available on the surface and that these active sites are not yet occupied/contaminated at the initial stage of the surface exposure to HONO.

Fig. 4 shows the concentrations of NO and NO_2 formed in the reaction of HONO with Al_2O_3 surface as a function of the consumed concentration of HONO. These results were observed with initial concentration of HONO varied in the range 1.2×10^{12} to 1.5×10^{13} molecule cm^{-3}. One can note that the impact of the initial concentration of HONO on the yield of the two detected products (determined as the ratio of the product concentration formed to the concentration of HONO consumed) was negligible. The straight lines in Fig. 4 correspond to the linear through origin fits to the experimental data and provide the branching ratios of 0.62 and 0.38 for the NO_2 and NO forming pathways, respectively.

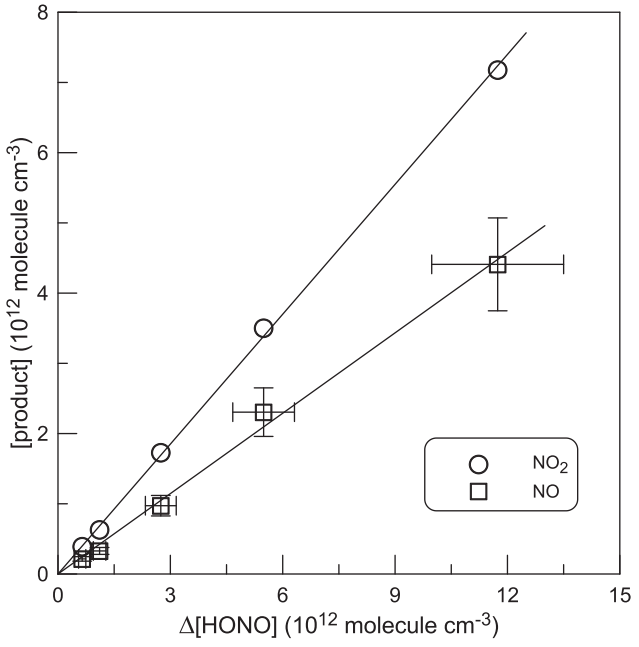

Fig. 4. Dependence of the concentration of the products (NO and NO_2) formed on the concentration of HONO consumed measured at $T = 300$ K under dry conditions and with initial concentration of HONO varied in the range (1.2–15.0) × 10^{12} molecule cm^{-3}. Error bars represent 15% uncertainty on the measurements of the respective concentrations.

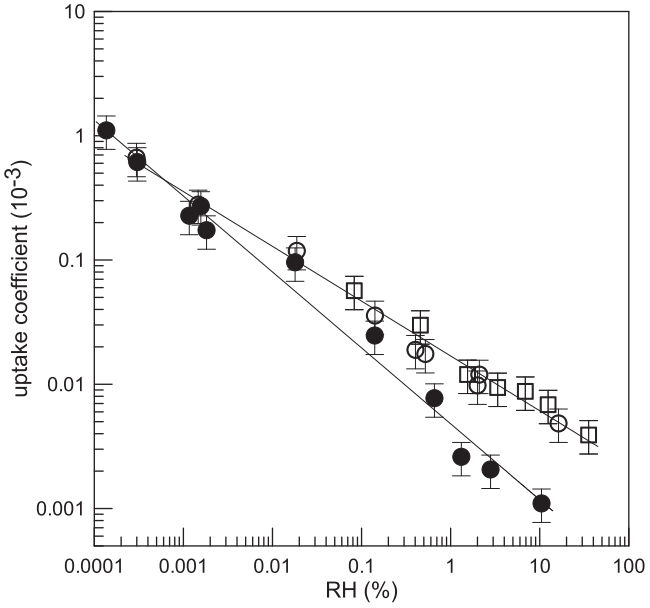

Fig. 5. Uptake coefficient as a function of relative humidity. Filled and open symbols correspond to the data measured under dark conditions and in the presence of irradiation, respectively. Circles and squares represent the respective results obtained at $T = 300$ and 280 K.

3.4. Dependence on relative humidity

In this series of experiments the uptake coefficient of HONO was measured as a function of relative humidity. Prior to uptake experiments (contact with HONO), the freshly prepared Al_2O_3 samples were heated under pumping (as noted in Section 2) and then exposed during nearly 5 min to water vapor present in the reactor. The measured uptake coefficient was found to be inversely dependent on the relative humidity (Fig. 5). The rather strong negative dependence observed for the uptake coefficient on RH under dark conditions (filled symbols) can be well represented by a power function (solid line in Fig. 5):

$$\gamma_{dark} = 4.8 \times 10^{-6}(RH)^{-0.61}$$

for RH in the range (1.4×10^{-4} to 10.5%) and with estimated conservative 30% uncertainty on the uptake coefficient determination.

The impact of water concentration on the yield of the reaction products was also explored. The results of the measurements are shown in Fig. 6 (filled symbols) as a dependence of the NO_2 and NO yields on relative humidity. The variation of the concentration of water by five orders of magnitude was found to have no impact on the products of the heterogeneous reaction.

3.5. Effect of UV irradiation

In contrast to the dry conditions, in presence of water in the reactor the UV irradiation of the Al_2O_3 film was found to increase the uptake coefficient of HONO. The relative contribution of the photo-initiated uptake of HONO to the total one increases with relative humidity (Fig. 5). As a result the dependence of the uptake coefficient on RH under irradiation is considerably weaker than that in dark:

$$\gamma_{photo} = 1.7 \times 10^{-5}(RH)^{-0.44}$$

for RH in the range (3.0×10^{-4} to 35.4%). Dependence of the uptake coefficient on the irradiation intensity was studied in additional experiments by switching on the different number of lamps in the reactor, from 1 to 6. This corresponds to the variation of the NO_2

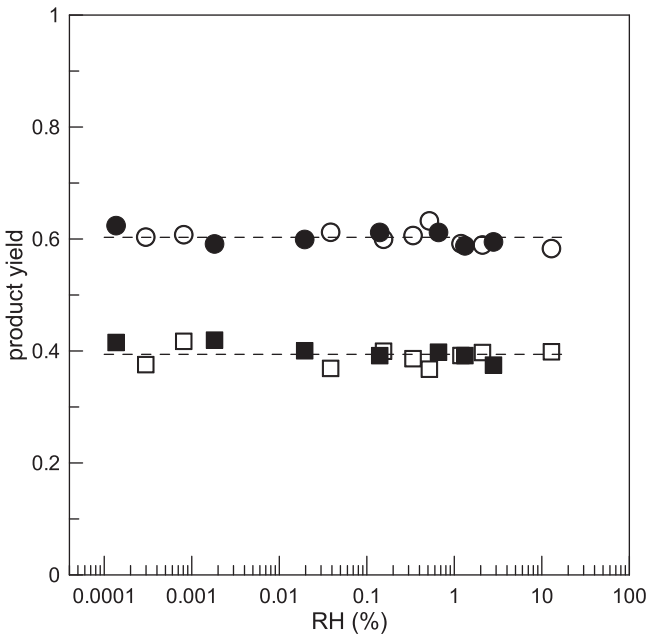

Fig. 6. Branching ratio of the NO (squares) and NO_2 (circles) forming pathways of the reaction of HONO with Al_2O_3 surface as a function of relative humidity. Filled and open symbols correspond to the data measured under dark conditions and in the presence of irradiation ($J_{NO_2} \cong 0.012\,s^{-1}$), respectively.

photolysis frequency from 0.002 to 0.012 s^{-1}. The results obtained at RH = 2.5% are shown in Fig. 7 (open symbols). A linear dependence of the heterogeneous loss rate of HONO on the irradiance intensity is clearly observed, with an intercept identical to the value of k' measured in absence of light.

Concerning the products of the heterogeneous reaction, the yields of NO and NO_2 were found to be independent of the irradiance intensity (Fig. 7) and identical to those observed under dark conditions (Fig. 6). The dashed lines in Fig. 6 correspond to the mean values obtained for NO_2 and NO yields: 0.60 and 0.39, respectively.

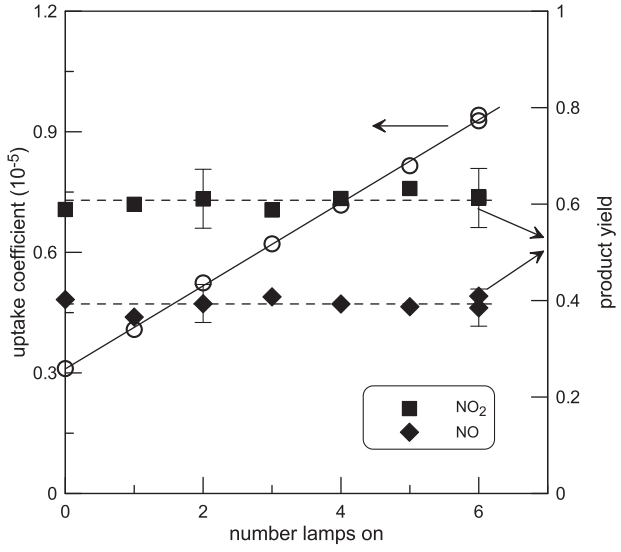

Fig. 7. Uptake coefficient of HONO on Al_2O_3 (open symbols) and product yield (filled symbols) as a function of the irradiation intensity (number of lamps switched on): T = 300 K, RH = 2.5%.

Table 2
Temperature dependence of the uptake coefficient of HONO on Al_2O_3 surface (RH ≈ 0.2%).

T (K)	Sample mass (mg cm^{-1})	$\gamma \times 10^5$ [a]
280	0.27	1.4
290	0.19	1.3
300	0.21	1.3
310	0.23	1.3
320	0.23	1.5

[a] Estimated uncertainty of 30%.

Table 3
Branching ratio of the NO_2 and NO forming pathways of the reaction of HONO with Al_2O_3 surface as a function of temperature.

T (K)	Branching ratio	
	NO_2	NO
275	0.61	0.41
280	0.61	0.39
285	0.61	0.40
290	0.63	0.40
295	0.60	0.39
300	0.60	0.41
305	0.62	0.40
310	0.60	0.40
315	0.61	0.42
320	0.62	0.38
320	0.63	0.42

3.6. Temperature dependence

Temperature dependence of the uptake coefficient of HONO on Al_2O_3 was measured in the temperature range (T = 280–320 K) at nearly 0.2% relative humidity. Such a low RH was caused by inability to reach higher relative humidity at high temperatures in the low pressure flow reactor used. Results of these experiments (Table 2) show that the uptake coefficient, $\gamma = (1.35 \pm 0.10) \times 10^{-5}$ is temperature independent in the range of a few percents statistical uncertainty and within the temperature range used.

The impact of temperature on the distribution of the reaction products was also found to be negligible (Table 3). The experimental data presented in Table 3 provide the mean values of 0.61 and 0.40 for the branching ratios of NO_2 and NO forming pathways, respectively, for the HONO reaction with aluminium oxide for temperatures between 275 and 320 K.

3.7. Surface adsorbed species

As one can see in Fig. 1, somewhat delayed product formation was observed in the first minutes of the Al_2O_3 exposure to HONO. This delayed formation of the products might be due to multiple reasons: (i) rapid initial non reactive uptake of HONO on limited number of specific active sites, (ii) relatively slow desorption of the products to the gas phase or (iii) their uptake to the reactive surface at the initial stage of the reaction, (iv) product formation in secondary surface reactions involving intermediates formed on the surface upon initial HONO uptake. In order to get additional information on the nature of the species remaining on the surface and not released into the gas phase during the heterogeneous reaction we have carried out additional experiments consisting in heating (up to 250 °C) or UV irradiation of the reacted (treated with HONO) samples of Al_2O_3 with simultaneous monitoring of the species emitted into the gas phase. In these experiments, the solid film of Al_2O_3 was first treated with HONO during a certain time, then pumped in a flow of helium and finally heated or irradiated. HONO and NO_2/NO were observed in the gas phase upon heating and UV irradiation of the reacted sample, respectively.

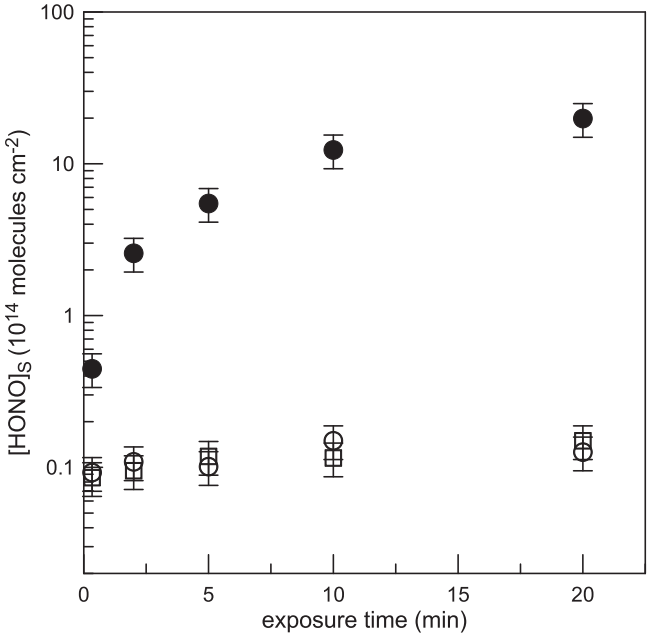

Fig. 8. Number of HONO molecules taken up by Al_2O_3 surface (filled circles) and HONO surface concentration (open symbols) as a function of exposure time at $T = 300$ K under dry conditions. Open circles and squares represent the results corresponding to Al_2O_3 exposure to HONO (1.4×10^{12} molecule cm^{-3}) under dark conditions and in presence of irradiation (6 lamps on), respectively.

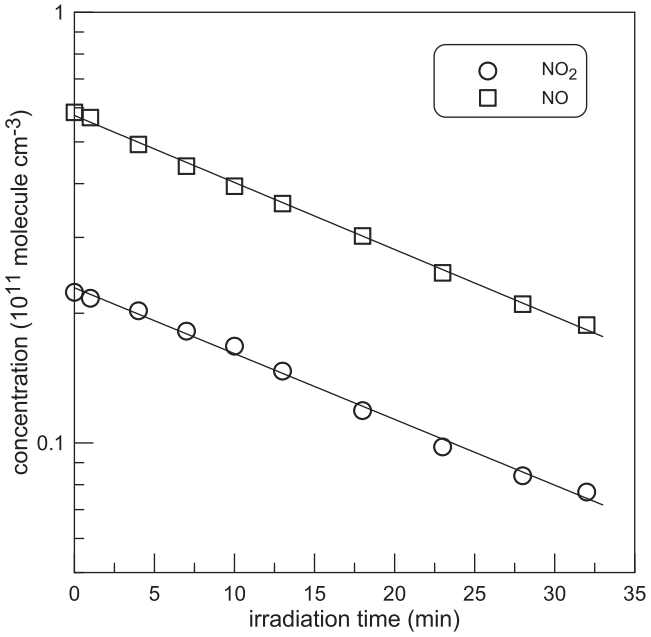

Fig. 9. Concentrations of NO and NO_2 observed in the gas phase upon UV irradiation (2 lamps switched on) of Al_2O_3 surface ($m = 0.8$ mg) previously exposed to [HONO] = 2×10^{12} molecule cm^{-3} during 20 min.

Fig. 8 shows the time dependence of the total number of HONO molecules lost on the surface (filled symbols) during heterogeneous interaction and surface concentration of non reacted HONO, remaining on the surface (open symbols), and determined via thermal desorption. The results presented in Fig. 8 correspond to two series of experiments carried out under dark conditions and on UV irradiated surface. As demonstrated above, the rates of HONO uptake under dry conditions were similar in the presence and in the absence of the UV irradiation, so the data shown in Fig. 8 for total HONO lost on the surface represent the mean values from two experiments. Concerning surface concentration of non reacted HONO, it was found to increase rapidly at the initial stage of the surface exposure to HONO (lowest exposure time was 20 s), and leveled off at a steady-state value of nearly 1.3×10^{13} mol cm^{-2} (calculated using BET surface area), regardless of whether the surface was irradiated or not during exposure to HONO. This steady state concentration of the surface HONO was found to be independent of temperature in the range 275–320 K. Another point which can be drawn from Fig. 8 is that at the initial stage of the heterogeneous reaction significant part of HONO (compared with the total HONO taken up) remains adsorbed on the surface, i.e. does not lead to the formation of the products in the gas phase. This fact seems to make clear the observed delayed formation of the reaction products in the gas phase.

Another set of experiments was devoted to analysis of species released into the gas phase upon UV irradiation in a flow of helium of the Al_2O_3 sample previously treated with HONO. Gaseous NO and NO_2 were observed upon surface irradiation with concentrations rapidly (a few seconds) reaching their maximum ($t = 0$ in Fig. 9) and then decreasing with time of irradiation. As shown in Fig. 9 the decrease of the concentrations of NO and NO_2 with time could be well described by an exponential function (solid lines) providing the value of 0.035 min^{-1} for the rates of both NO and NO_2 concentrations decrease (with 2 UV lamps switched on, $J_{NO_2} = 0.004\ s^{-1}$). Assuming that desorption of NO and NO_2 is much more rapid process compared with their production reaction on the surface, the measured rate of the decrease of the NO and NO_2 concentrations in the gas phase can be attributed to the consumption of the surface reactant leading to the formation of these two products. Fig. S2, Supplementary data presents the results of similar experiments carried out under irradiation with 6 UV lamps. Exponential fit of the observed profiles of NO and NO_2 provides the values of 0.097 and 0.103 min^{-1} for the rates of decrease of NO and NO_2 concentrations with time, respectively. Comparing with the data observed with 2 UV lamps, one can note that increase of the irradiation intensity by a factor of 3 leads to similar increase in the rate of heterogeneous reaction, indicating its photolytic nature. Two points can be noted regarding the data presented in Fig. 9 and Fig. S2. Firstly, the concentration of NO is by a factor of nearly 3 higher than the concentration of NO_2, i.e. differs greatly from the distribution of the products observed in reaction of HONO with Al_2O_3 surface. It should be noted at this point, that the observed photolytic production of NO and NO_2 is negligible compared with concentrations of these species generated in the experiments in the presence of HONO in the gas phase and could not impact the measurements of the products yields reported above. Secondly, the integrated number of NO and NO_2 molecules emitted into the gas phase upon surface irradiation is nearly 4×10^{13} mol cm^{-2} (normalized by surface area), i.e. significantly higher than the HONO concentration available on the surface (1.3×10^{13} mol cm^{-2}). These observations seem to indicate that other, than HONO, species are present on the HONO treated surface and/or are formed via HONO/surface interaction upon heating. Indeed, a peak at $m/z = 46$ was detected by mass spectrometry upon heating of the reacted sample of Al_2O_3. This peak could correspond to desorbed NO_2 but also to nitric acid which is another plausible candidate for the missing surface adsorbed species. Although no signal was observed at $m/z = 63$ (HNO_3^+) upon sample heating, a peak at $m/z = 46$ could be due to fragmentation of HNO_3 in the ion source of the mass spectrometer, the signal intensity of the NO_2^+ fragment of HNO_3 being by nearly two orders of magnitude higher than that of the parent peak [22]. Unfortunately, in the frame of this study we had no possibility to directly detect and quantify HNO_3 probably present on the reactive surface (by ion chromatography, for example).

4. Discussion

In the present study, two gas phase products, NO_2 and NO, were found to be formed in the heterogeneous reaction of HONO with Al_2O_3 surface with yields of 60 ± 9 and $40 \pm 6\%$, respectively. The branching ratios for the NO and NO_2 forming reaction pathways were shown to be independent of temperature ($T = 275$–320 K), relative humidity (1.4×10^{-4} to 12.9%) and UV irradiation. Similar results were observed in our previous study of the interaction of HONO with TiO_2 surface under dark conditions [20]. Syomin and Finlayson-Pitts [16] reported equal yields for NO and NO_2 from reaction of HONO with unconditioned glass cell under dry conditions. The formation of equal amounts of NO and NO_2 was suggested to proceed via autoionization reaction between gas-phase and adsorbed HONO:

$$HONO_g + HONO_{ads} \rightarrow NO^+ + NO_2^- + H_2O$$

$$NO^+ + NO_2^- \rightarrow N_2O_3 \rightarrow NO + NO_2$$

The present observation of the steady state for the surface adsorbed HONO together with the nearly unity total yield for the sum of the gas phase products, can be interpreted as an evidence that initially adsorbed HONO does not accumulate on the surface and is involved in secondary reactions leading to the observed gas phase products in accordance with the above mechanism. However, non equal yields of NO and NO_2 observed in the present study seem to indicate that other reactive processes can also occur in the interaction of HONO with Al_2O_3 surface, for instance, oxidation/reduction reactions like those proposed in our recent study for HONO + TiO_2 reaction [20]:

$$HONO + SS \rightarrow NO_2 + H^+ + \text{reduced SS}$$

$$HONO + H^+ + \text{reduced SS} \rightarrow NO + H_2O + SS,$$

where SS denotes surface site. The possible secondary transformation of NO_2 formed on the surface can also influence the final distribution of the reaction products in the gas phase and should not be disregarded.

HONO and another species with a peak at $m/z = 46$ were observed in the gas phase upon heating of the Al_2O_3 sample previously reacted with HONO. Unfortunately, we were not able to distinguish between NO_2 and possible HNO_3 fragment contributions to the signal at mass 46. It was also observed that upon UV irradiation of the treated with HONO sample of Al_2O_3, NO and NO_2 were released from the surface into the gas phase. In this respect, it can be noted that Zhou et al. [23] have detected the formation of gaseous HONO, NO_2 and NO upon UV irradiation of a Pyrex surface coated with HNO_3. The effect was attributed to HNO_3 photolysis on the surface. Schuttlefield et al. [24] and Rubasinghege and Grassian [25] observed NO and NO_2 and N_2O formation upon irradiation of nitric acid-reacted alumina (γ-Al_2O_3). The gas-phase product distribution was observed to be dependent on environmental conditions. Thus NO was found as a major product in the absence of oxygen in the reactive system. Our data on irradiation of HONO-reacted alumina are in line with this observation. Zhou et al. [23] reported a heterogeneous HNO_3 photolysis rate of 6×10^{-5} s^{-1} for noontime sun under dry conditions. The HNO_3 photolysis rates estimated by Rubasinghege and Grassian [25] were in the range $(3.2$–$5.6) \times 10^{-5}$ s^{-1} for RH in the range (<1–80%). These values are much lower compared with the consumption rate of the surface reactant (1.8×10^{-3} s^{-1}) measured in the present study from the time profiles of NO and NO_2 in the gas phase upon irradiation (6 lamps, $J_{NO_2} = 0.012$ s^{-1}) of treated with HONO Al_2O_3 surface. In addition, in thermal desorption experiments we have verified that nearly 65% of surface HONO was consumed upon irradiation (6 lamps) during 10 min, i.e. with the rate similar to that measured from the profiles of NO and NO_2 released to the gas phase. All these considerations seem to indicate that for the studies discussed herein surface nitrate is not involved in the chemistry observed on Al_2O_3 samples previously exposed to HONO and the mass spectrometric signal observed at $m/e = 46$ upon heating of the reacted surface belongs to NO_2. This gaseous NO_2 could result from the surface adsorbed NO_2, but most likely from the reaction of HONO released by heating the surface.

UV irradiation of the reactive surface was found to increase its reactivity. The contribution of the UV irradiation to the uptake coefficient is dependent on relative humidity, being negligible under dry conditions and more pronounced at high RH (Fig. 5). It is difficult to discuss the mechanism of the photoreaction of HONO with Al_2O_3 at this stage. From one side, the yields of the reaction products, NO_2 and NO, were found to be independent of the irradiation intensity and similar to those under dark conditions. From another side, experiments with irradiation of the reacted surface have shown that reaction intermediates on the surface were photolabile and could be transformed into gaseous NO and NO_2 via their photolysis and/or photoinitiated surface reactions, however with product yields which differed from those observed in presence of HONO in the reactive system. Another point is that the photo-induced reaction of HONO on Al_2O_3 surfaces should not be considered as due to photocatalytic activation of the surface, since alumina is an insulator material not absorbing UV-A radiation. Hence, the direct band gap excitation of Al_2O_3 under our experimental conditions is excluded. The observed phenomenon can be attributed to the surface mediated photodegradation of HONO on Al_2O_3 via the mechanism similar to that proposed by Karunakaran et al. [26] for the photodegradation of organic acids (formic, acetic, oxalic and citric acids) on γ-Al_2O_3 and SiO_2 surfaces. According to the proposed mechanism, the chemisorbed carboxylic acids absorb the UV-A irradiation and transfer an electron to the surface Al^{3+} and Si^{4+} sites. This was suggested to be the initial step of the process, the rest of the mechanism being similar to that in semiconductor photocatalysis [26]. Similar observations have been also reported for semiconductor materials. It was shown, for example, that 2,4,5-trichlorophenol forms a charge transfer complex with TiO_2 resulting in the surface activation under sub-band-gap illumination at wavelength as long as 520 nm [27].

Rather strong inverse dependence on relative humidity was found for the uptake coefficient of HONO to Al_2O_3 surface in the present study: $\gamma \sim [RH]^{-0.61}$ and $[RH]^{-0.44}$ under dark and irradiation conditions, respectively. In a recent study from our group [20], similar dependence was observed for the interaction of HONO with TiO_2 surface under dark conditions, $\gamma = 1.8 \times 10^{-5}\,(RH)^{-0.63}$, although the absolute values of the uptake coefficient of HONO on TiO_2 surface were by a factor of nearly 4 higher compared with those on Al_2O_3. Similar effect of the decrease of the HONO loss rate with increasing RH was observed in previous studies carried out with glass surfaces [14,16]. Moreover, in the work of Kaiser and Wu [14] the rate of HONO loss on the walls of a Pyrex reactor was found to decrease with increasing RH (from 0.2 to 5%) in accordance with an apparent reaction order in water concentration of −0.6, which is identical to our data for TiO_2 [20] and Al_2O_3 (this study). The negative dependence of the HONO uptake rate on water concentration was attributed to competition between HONO and H_2O for the available surface sites [16]. It is noteworthy that the RH dependences are quite different for the uptake of nitrous and nitric acids. Thus Goodman et al. [28] studying kinetics of nitric acid uptake on oxide particles, observed an enhancement in the uptake coefficient upon increase of the relative humidity.

The results obtained for the uptake of HONO on Al_2O_3 surface can be discussed in relation to atmospheric HONO chemistry occurring on aerosols and different types of ground surfaces. Concerning

dark reaction, in our recent study the potential loss of HONO on aerosol surface was estimated using the experimental data for TiO_2 (for 40% RH) and compared with HONO loss due to dry deposition which is the main HONO sink process during night-time [20]. It was shown that the calculated rate of HONO loss on aerosols is much lower (at least by a factor of 50) than the dry deposition rate of HONO. Considering that the uptake coefficient of HONO to Al_2O_3 is by a factor of nearly 4 lower compared with TiO_2, the uptake data from the present study would result in even lower nocturne loss rates of HONO. The experimental data obtained in the present study for HONO uptake on UV irradiated surface of Al_2O_3 can be applied to assess the potential role of HONO loss on mineral aerosols during daytime. Using the value of $\gamma(UV) = 4 \times 10^{-6}$ measured at 30% RH with 6 UV lamps switched on ($J_{NO_2} = 0.012\,s^{-1}$, clear sky conditions) [29], aerosol surface loading of 10^{-6} to 10^{-5} cm^{-1} [30,31], typical for rural and urban atmosphere and in accordance with

$$k' = \frac{\omega\gamma}{4}\frac{S}{V}$$

the calculated value of HONO loss rate on aerosols is: $k' \sim 3 \times 10^{-8}$ to 3×10^{-7} s^{-1} (for RH = 30%, T = 300 K). As one could expect, these numbers are negligible compared to the photolysis rate of HONO of $\sim 1.3 \times 10^{-3}$ s^{-1} [29]. Thus the contribution of aerosol to the total HONO loss in the atmosphere either during the day and night-time can be considered as negligible.

Acknowledgements

This study was supported by LEFE – CHAT programme of CNRS (Photona project) and ANR from Photodust grant. A.E.Z. is very grateful to région Centre for financing his PhD grant.

Appendix A. Supplementary data

Supplementary data associated with this article can be found, in the online version, at http://dx.doi.org/10.1016/j.jphotochem.2012.09.018.

References

[1] J. Calvert, G. Yarwood, A. Dunker, An evaluation of the mechanism of nitrous acid formation in the urban atmosphere, Research on Chemical Intermediates 20 (1994) 463–502.
[2] M. Kerbrat, T. Huthwelker, H.W. Gäggeler, M. Ammann, Interaction of nitrous acid with polycrystalline ice: adsorption on the surface and diffusion into the bulk, Journal of Physical Chemistry C 114 (2010) 2208–2219.
[3] G. Lammel, J.N. Cape, Nitrous acid and nitrite in the atmosphere, Chemical Society Reviews 25 (1996) 361–369.
[4] B.R. Appel, A.M. Winer, Y. Tokiwa, H.W. Biermann, Comparison of atmospheric nitrous acid measurements by annular denuder and differential optical absorption systems, Atmospheric Environment Part A: General 24 (1990) 611–616.
[5] S.-M. Li, Equilibrium of particle nitrite with gas phase HONO: tropospheric measurements in the high Arctic during polar sunrise, Journal of Geophysical Research 99 (1994) 25469–25478.
[6] Z. Vecera, P.K. Dasgupta, Measurement of ambient nitrous acid and a reliable calibration source for gaseous nitrous acid, Environmental Science and Technology 25 (1991) 255–260.
[7] J. Kleffmann, Daytime sources of nitrous acid (HONO) in the atmospheric boundary layer, ChemPhysChem 8 (2007) 1137–1144.
[8] L. Chu, G. Diao, L.T. Chu, Heterogeneous interaction and reaction of HONO on ice films between 173 and 230 K, Journal of Physical Chemistry A 104 (2000) 3150–3158.
[9] G. Diao, L.T. Chu, Heterogeneous reactions of HX + HONO and I_2 on ice surfaces: kinetics and linear correlations, Journal of Physical Chemistry A 109 (2005) 1364–1373.
[10] F.F. Fenter, M.J. Rossi, Heterogeneous kinetics of HONO on H_2SO_4 solutions and on ice: activation of HCl, Journal of Physical Chemistry 100 (1996) 13765–13775.
[11] M. Kerbrat, T. Huthwelker, T. Bartels-Rausch, H.W. Gaggeler, M. Ammann, Co-adsorption of acetic acid and nitrous acid on ice, Physical Chemistry Chemical Physics 12 (2010) 7194–7202.
[12] S. Lelièvre, Y. Bedjanian, G. Laverdet, G. Le Bras, Heterogeneous reaction of NO_2 with hydrocarbon flame soot, Journal of Physical Chemistry A 108 (2004) 10807–10817.
[13] D. Stadler, M.J. Rossi, The reactivity of NO_2 and HONO on flame soot at ambient temperature: the influence of combustion conditions, Physical Chemistry Chemical Physics 2 (2000) 5420–5429.
[14] E.W. Kaiser, C.H. Wu, A kinetic study of the gas phase formation and decomposition reactions of nitrous acid, Journal of Physical Chemistry 81 (1977) 1701–1706.
[15] H.M. Ten Brink, H. Spoelstra, The dark decay of HONO in environmental (SMOG) chambers, Atmospheric Environment 32 (1998) 247–251.
[16] D.A. Syomin, B.J. Finlayson-Pitts, HONO decomposition on borosilicate glass surfaces: implications for environmental chamber studies and field experiments, Physical Chemistry Chemical Physics 5 (2003) 5236–5242.
[17] Y. Bedjanian, S. Lelièvre, G. Le Bras, Experimental study of the interaction of HO_2 radicals with soot surface, Physical Chemistry Chemical Physics 7 (2005) 334–341.
[18] A. El Zein, Y. Bedjanian, Interaction of NO_2 with TiO_2 surface under UV irradiation: measurements of the uptake coefficient, Atmospheric Chemistry and Physics 12 (2012) 1013–1020.
[19] Y. Bedjanian, S. Lelièvre, G.L. Bras, Kinetic and mechanistic study of the F atom reaction with nitrous acid, Journal of Photochemistry and Photobiology A 168 (2004) 103–108.
[20] A. El Zein, Y. Bedjanian, Reactive uptake of HONO to TiO_2 surface: "dark" reaction, Journal of Physical Chemistry A 116 (2012) 3665–3672.
[21] G.M. Underwood, P. Li, C.R. Usher, V.H. Grassian, Determining accurate kinetic parameters of potentially important heterogeneous atmospheric reactions on solid particle surfaces with a Knudsen Cell Reactor, Journal of Physical Chemistry A 104 (2000) 819–829.
[22] F.F. Fenter, F. Caloz, M.J. Rossi, Heterogeneous kinetics of N_2O_5 uptake on salt, with a systematic study of the role of surface presentation (for N_2O_5 and HNO_3), Journal of Physical Chemistry 100 (1996) 1008–1019.
[23] X. Zhou, H. Gao, Y. He, G. Huang, S.B. Bertman, K. Civerolo, J. Schwab, Nitric acid photolysis on surfaces in low-NO_x environments: significant atmospheric implications, Geophysical Research Letters 30 (2003) 2217.
[24] J. Schuttlefield, G. Rubasinghege, M. El-Maazawi, J. Bone, V.H. Grassian, Photochemistry of adsorbed nitrate, Journal of the American Chemical Society 130 (2008) 12210–12211.
[25] G. Rubasinghege, V.H. Grassian, Photochemistry of adsorbed nitrate on aluminum oxide particle surfaces, Journal of Physical Chemistry A 113 (2009) 7818–7825.
[26] C. Karunakaran, R. Dhanalakshmi, G. Manikandan, P. Gomathisankar, Photodegradation of carboxylic acids on Al_2O_3 and SiO_2 nanoparticles, Indian Journal of Chemistry 50A (2011) 163–170.
[27] A.G. Agrios, K.A. Gray, E. Weitz, Photocatalytic transformation of 2,4,5-trichlorophenol on TiO_2 under sub-band-gap illumination, Langmuir 19 (2003) 1402–1409.
[28] A.L. Goodman, E.T. Bernard, V.H. Grassian, Spectroscopic study of nitric acid and water adsorption on oxide particles: enhanced nitric acid uptake kinetics in the presence of adsorbed water, Journal of Physical Chemistry A 105 (2001) 6443–6457.
[29] A. Kraus, A. Hofzumahaus, Field measurements of atmospheric photolysis frequencies for O_3, NO_2, HCHO, CH_3CHO, H_2O_2, and HONO by UV spectroradiometry, Journal of Atmospheric Chemistry 31 (1998) 161–180.
[30] J.H. Seinfeld, S.N. Pandis, Atmospheric Chemistry and Physics, Wiley-Interscience, New York, 1998.
[31] B. Wehner, A. Wiedensohler, Long term measurements of submicrometer urban aerosols: statistical analysis for correlations with meteorological conditions and trace gases, Atmospheric Chemistry and Physics 3 (2003) 867–879.